

# Solvent Effects on the Complex Formation of Benzophenone Ketyl Radical and Triethylamine

Toyohiko Abe, Akio Kawai, Yoshizumi Kajii,<sup>†</sup> Kazuhiko Shibuya,\* and Kinichi Obi<sup>‡</sup>

Department of Chemistry, Graduate School of Science and Engineering, Tokyo Institute of Technology, 2-12-1 Ohokayama, Meguro, Tokyo 152-8551, Japan

Received: October 12, 1998; In Final Form: January 15, 1999

The 1:1 complex formation between benzophenone ketyl radical (BPK) and triethylamine in various solvents was studied by means of nanosecond laser flash photolysis. The complex shows an absorption band slightly red-shifted from that of uncoupled BPK. The formation constants ( $K_f$ 's) were determined from the absorbance change of the complex against amine concentration. The  $K_f$  values are in the range 60–103 M<sup>-1</sup> depending on the dielectric constant of solvent ( $\epsilon_r = 10.7$ –1.89). Enthalpy and entropy changes in the complex formation reactions were determined from van't Hoff plots around room temperature. The measured enthalpy change of  $-2.0$  to  $-7.5$  kcal mol<sup>-1</sup> depends on  $\epsilon_r$ , which is explained with an Onsager's reaction field theory. The measured entropy change varies from  $-16.5$  cal K mol<sup>-1</sup> to nearly zero, and the dependence on the solvent is discussed in terms of the solvation effect.

## 1. Introduction

Benzophenone ketyl (BPK) radical is well-known as a product in the photoreduction of benzophenone. Many groups have studied reaction mechanisms of benzophenone in the condensed phase<sup>1–19</sup> and in the gas phase.<sup>20,21</sup> The dynamics of BPK has also absorbed much interest.<sup>22–29</sup> The visible absorption spectrum of BPK shows a broad 500–570 nm band with a peak at 545 nm. This broad band slightly red-shifts in the presence of aliphatic amine. Kajii et al. concluded that this spectral shift is due to the complex formation of BPK with aliphatic amines such as triethylamine (TEA) and *sec*-butylamine.<sup>26</sup> The complex formation of ketyl type radicals was originally suggested by Davidson and Wilson from the analysis of the ESR spectra in the presence of amines.<sup>22</sup> The hyperfine coupling constant of hydrogen atom in the hydroxy group ( $a_{OH}$ ) of ketyl increased when amine concentration increased, which led them to a conclusion that ketyl formed a complex or some sort of solvated radical with amine. However, no quantitative analysis on the complex had been carried out until the laser flash photolysis study by Kajii et al. was done.<sup>26</sup>

BPK forms a 1:1 complex with TEA.<sup>26</sup> This chemical formula may hold for complexes of other ketyl type radicals and aliphatic amines, since the ketyl radical has a hydroxy group that can form a hydrogen bond with amine. A time-resolved ESR study also indicates that  $\alpha$ -hydroxybenzyl radical forms a 1:1 complex with various aliphatic amines.<sup>27</sup> The complexes of BPK or  $\alpha$ -hydroxybenzyl radical with amines have  $a_{OH}$  values larger than those of the corresponding uncoupled ketyl type radicals.<sup>22,27</sup> The spectral shift in the visible absorption band of BPK upon complex formation is quite small, about 330 cm<sup>-1</sup>.<sup>26</sup> These results suggest that the complex is formed through the hydrogen bond between hydroxy and amino groups.

In the present study, we clarify that the complex formation constant  $K_f$  does not depend on the ionization potential (IP) of amine, which excludes the possibility of charge-transfer interaction in the complex formation and confirms the hydrogen bond mechanism. Another purpose of this study is to elucidate how solvent affects the complex formation. The  $K_f$  value depends strongly on the dielectric constant ( $\epsilon_r$ ) of the solvent, while no dependence was found on viscosity. The van't Hoff plot gives the enthalpy and entropy changes ( $\Delta H$  and  $\Delta S$ ) of the complex formation reaction. The  $\Delta H$  varies from  $-2.0$  to  $-7.5$  kcal mol<sup>-1</sup>, and these values seem reasonable for hydrogen bonds.<sup>29,30</sup> The  $\epsilon_r$  dependence of  $\Delta H$  is explained by Onsager's reaction field theory;<sup>32–34</sup> the  $\Delta H$  value shows a linear dependence on  $(\epsilon_r - 1)/(\epsilon_r + 2)$ . The  $\Delta S$  value varies from  $-16.5$  cal K mol<sup>-1</sup> to nearly zero, and the solvent dependence is discussed in terms of solvation effect.

## 2. Experimental Section

Details of a transient absorption detection system have already been described elsewhere.<sup>13</sup> A XeCl excimer laser (Lambda Physik LPX, 308 nm, 20 ns duration time) was used as an excitation light source at a repetition rate of 1 Hz. A Xe flash lamp (Ushio UXL150DS, 150 W) was synchronously fired with the excimer laser pulse to monitor transient species produced by the photolysis laser and operated with a pulse duration time of about 200  $\mu$ s, which enabled us to study microsecond-order chemical kinetics. The monitoring light was detected with a monochromator (Nikon P250)/photomultiplier tube (Hamamatsu Photonics R928) combination system, which had a spectral resolution of 2 nm. The transient absorption signals were digitized by a digital memory (Iwatsu DM901) and analyzed by a personal computer. The transient signals were accumulated over 30 times to improve the S/N ratio.

Benzophenone (Tokyo Kasei; GR grade) was recrystallized a few times from ethanol.  $\alpha$ -Phenylbenzoin was synthesized by the Grignard reaction of phenylmagnesium bromide with

<sup>†</sup> Research Center for Advanced Science and Technology, The University of Tokyo, 4-6-1 Komaba, Meguro, Tokyo 153-0041, Japan.

<sup>‡</sup> Department of Chemical and Biological Sciences, Japan Women's University, 2-8-1 Mejirodai, Bunkyo-ku, Tokyo 112-8681, Japan.

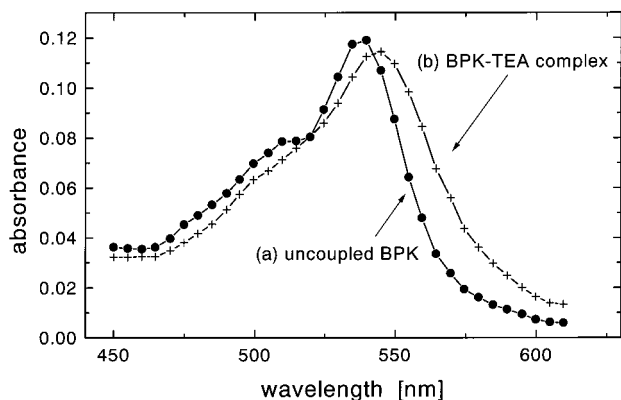


**Figure 1.** Transient absorption spectra of (a) BPK and (b) BPK/TEA complex obtained for the benzophenone/TEA system in cyclohexane. The concentrations of TEA were (a) 6.25 and (b) 100 mM. The spectra were measured at 0.8  $\mu$ s after laser excitation.

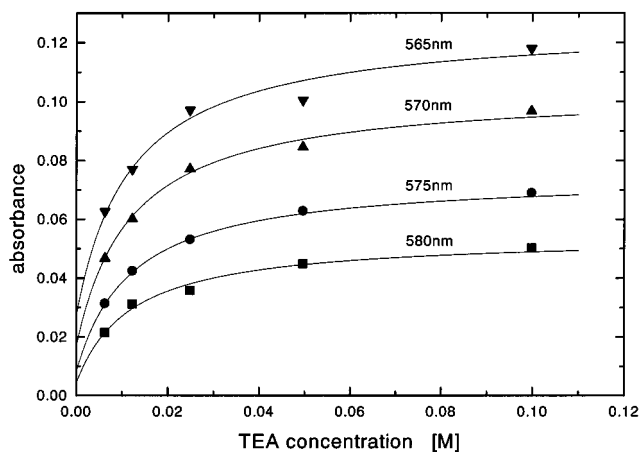


**Figure 2.** Plots of absorbance vs TEA concentration in cyclohexane. The formation constant ( $K_f$ ) and the molar extinction coefficient of the complex ( $\epsilon_c$ ) were obtained by fitting the eq 1 to the plots.

benzil in tetrahydrofuran at 245 K and recrystallized from *n*-hexane. All solvents were purchased from Kanto Chemical (GR-grade) and used as received. Triethylamine (Kanto Chemical; TCL grade) was distilled in a high-vacuum line. All samples were deaerated by bubbling solvent-saturated Ar gas. The temperature of the sample solution was controlled with a water bath, and the solution was flowed into a quartz cell at a flow rate of about 20 mL  $\text{min}^{-1}$ . The temperature of the solution was monitored with the thermocouples attached on the quartz cell.

### 3. Results and Discussion

**3.1. Formation Constants of BPK/TEA Complex in Various Solvents.** Figure 1 shows the transient absorption spectra of BPK obtained at 0.8  $\mu$ s delay following 308 nm laser photolysis of a benzophenone/TEA system in cyclohexane. The hydrogen abstraction reaction of triplet benzophenone from TEA yields BPK and the corresponding TEA radical. The absorption spectrum in Figure 1a shows a broad band with a peak at 540 nm and a shoulder at 510 nm, which are characteristic of uncoupled BPK. The spectral shape depended on TEA concentration. Spectrum a changed to the spectrum b when the TEA concentration increased 16 times. Spectrum b is dominated by the complex of BPK and TEA according to the previous work.<sup>26</sup> The complex band is slightly red-shifted and broader compared to that of uncoupled BPK. This red shift of the complex has

**TABLE 1: Formation Constants of BPK/TEA Complex in Various Solvents at 293 K**

solvent	$\eta$ [cP]	$\epsilon_r$	$K_f$ [ $\text{M}^{-1}$ ]	$\Delta G$ [kcal $\text{mol}^{-1}$ ]
<i>n</i> -hexane	0.31	1.89	103	-2.70
<i>n</i> -heptane	0.41	1.92	101	-2.69
cyclohexane	0.98	2.02	99	-2.68
methylcyclohexane	0.69	2.02	98	-2.67
benzene	0.65	2.28	37	-2.10
<i>o</i> -chlorotoluene		4.45	83	-2.57
<i>p</i> -chlorotoluene		6.08	70	-2.47
1,2-dichloroethane	0.80	10.7	60	-2.38

been explained on the basis of a conventional polar solvent effect on the  $\pi\pi^*$  transition, since the absorption around 540 nm is assigned to the  $\pi\pi^*$  transition.<sup>26</sup> The triplet-triplet absorption of benzophenone could not be measured in the present experiment with a long delay time of 0.8  $\mu$ s because triplet benzophenone decays in 10 ns through a fast hydrogen abstraction reaction.

In the present study, we measured the complex formation constant,  $K_f$ , in various solvents. It should be noted that the complex band was not always recognized in the 308 nm laser photolysis of the benzophenone/TEA system; in polar solvents with dielectric constants larger than 11, the benzophenone anion was produced instead of BPK or the amine complex. We performed all the experiments using solvents with dielectric constants smaller than 11.

The experimental procedures to determine the formation constant have been described in the previous paper.<sup>26</sup> We made a minor modification. The  $K_f$  value follows the equation

$$K_f = \frac{[C]}{[\text{BPK}][\text{TEA}]}$$

where C represents the complex. The OD value at a wavelength  $\lambda$  is given by  $\text{OD}(\lambda) = \epsilon_k[\text{BPK}] + \epsilon_c[C]$  where  $\epsilon_k$  and  $\epsilon_c$  are the molar extinction coefficients of BPK and the complex, respectively. We introduce a constant  $\alpha$ , which is equal to the concentration of  $[\text{BPK}] + [C]$ . As long as the initial concentration of benzophenone and the excitation laser power are kept constant,  $\alpha$  is a constant value. Hence, the final form of  $\text{OD}(\lambda)$  is given by the equation

$$\begin{aligned} \text{OD}(\lambda) &= \frac{\epsilon_k \alpha}{1 + K_f[\text{TEA}]} + \frac{\epsilon_c K_f [\text{TEA}] \alpha}{1 + K_f[\text{TEA}]} \\ &= \alpha \epsilon_c \frac{K_f [\text{TEA}] + \frac{\epsilon_k}{\epsilon_c}}{1 + K_f[\text{TEA}]} \end{aligned} \quad (1)$$

To determine  $K_f$  and  $\epsilon_c$  values from eq 1, we measured  $\text{OD}(\lambda)$  at six wavelengths against TEA concentration as shown in Figure 2. The  $K_f$  and  $\epsilon_c$  values for the BPK/TEA system in cyclohexane were determined from the least-squares fit of eq 1 to the results shown in Figure 2 using the molar extinction coefficient  $\epsilon_k = 4600 \text{ M}^{-1} \text{ cm}^{-1}$  at the peak (540 nm).<sup>4</sup> The averaged value of six  $K_f$ 's was adopted as the final  $K_f$  value in cyclohexane. We obtained similar fitting curves for several solvents, and the results are summarized in Table 1.

**3.2. Bond in BPK/TEA Complex.** The absorption spectrum of the BPK/TEA complex shows a red shift when the solvent is changed from nonpolar to polar. On the basis of the spectral shift, we examined two possible types of complexes, hydrogen-bonded and charge-transfer (CT) complexes. The visible absorp-

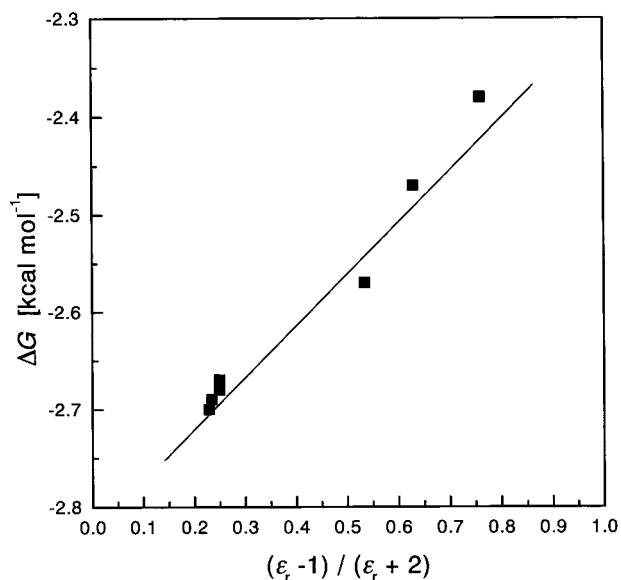


**Figure 3.** Correlation between  $\Delta G$  and  $(\epsilon_r - 1)/(\epsilon_r + 2)$  at room temperature. Solvents used are *n*-hexane, *n*-heptane, cyclohexane, methylcyclohexane, *o*-chlorotoluene, *p*-chlorotoluene, and 1,2-dichloroethane. Data are fitted to a linear relation.

tion band of the BPK/TEA complex is red-shifted by about  $330 \text{ cm}^{-1}$  from that of uncoupled BPK. Since the spectral shift of CT complexes is generally more than  $1000 \text{ cm}^{-1}$ ,<sup>35</sup> the spectral shift in the present system may be understood as a hydrogen-bond complex. Moreover, the CT complex model is also excluded by the following experiments. The spectral changes and the variation in  $K_f$  were studied for a series of pyridines as amines with different ionization potentials (IP). In these experiments BPK was prepared by the XeCl excimer laser photolysis of  $\alpha$ -phenylbenzoin, since the reaction efficiency to generate BPK in the BP/pyridine system is too low to detect BPK by the transient absorption technique. The  $K_f$  values obtained were 99, 89, 92, and 102 for pyridine (IP = 9.4–9.7 eV), 2-methylpyridine (9.2 eV), 2,6-dimethylpyridine (8.9–9.2 eV), and 2,4,6-trimethylpyridine (8.9 eV), respectively.<sup>36</sup> It can be seen that the  $K_f$  value is constant for any pyridines with different IP. Furthermore, if this complex is formed through CT interaction, the spectrum is expected to shift to red with a decrease in the IP value of amine (electron donor), but actually no spectral shift was observed. These experimental observations lead us to conclude that BPK and TEA do not form a CT complex but a hydrogen-bonded complex, which is consistent with the conclusion derived from the ESR measurements of the complex.<sup>22,27</sup>

**3.3. Factors Determining Formation Constant.** Table 1 lists the  $K_f$  values measured in eight solvents, together with their viscosity coefficient ( $\eta$ ) and dielectric constant ( $\epsilon_r$ ). It is quite clear from Table 1 that the formation constant depends on solvent. We discuss factors determining the formation constant of hydrogen-bonded BPK/TEA complex on the basis of solvent properties,  $\eta$  and  $\epsilon_r$ .

The viscosity of the solvent is an important property to control chemical reactions in solution. The viscosity determines the diffusional motion of the solute in solution, which may affect both the formation and dissociation rates of the complexes. In the present systems, the  $K_f$  values are almost constant around  $100 \text{ M}^{-1}$  in the viscosity range from 0.31 (*n*-hexane) to 0.98 (cyclohexane). This observation excludes the solvent viscosity as an important factor determining  $K_f$  in the present systems.

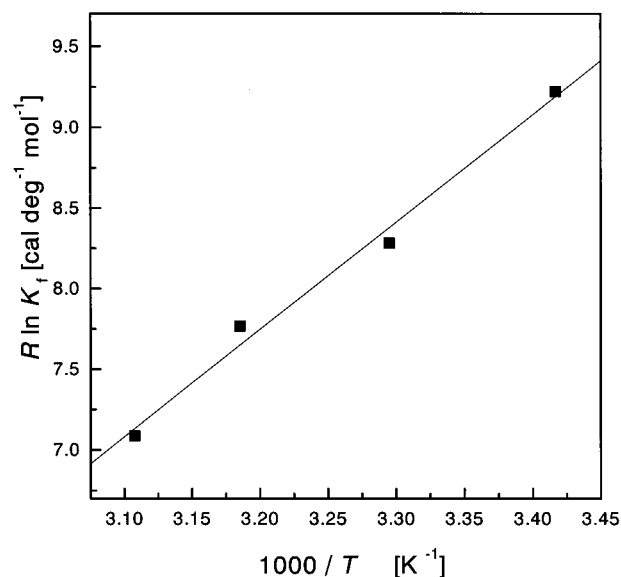


**Figure 4.** van't Hoff plot for the BPK/TEA complex formation reaction in *n*-hexane. The  $\Delta H$  and  $\Delta S$  values were determined from the slope and the intercept, respectively.

Next we discuss the effect of dielectric constant of solvent. The  $K_f$  value in *n*-hexane ( $\epsilon_r = 1.89$ ) is  $103 \text{ M}^{-1}$ , while that in 1,2-dichloroethane ( $\epsilon_r = 10.7$ ) is  $60 \text{ M}^{-1}$  as shown in Table 1. This implies that the dielectric constant of the solvent plays an important role in determining  $K_f$ . In Table 1, one finds a correlation; the larger the dielectric constant is, the smaller the  $K_f$  value is. It is thus concluded that the dielectric constant of the solvent controls the  $K_f$  value. It was reported<sup>26</sup> that  $K_f$  in benzene showed an exceptionally small value,  $37 \text{ M}^{-1}$ . This may be due to the peculiar solvent cage effect of benzene, but we cannot find any plausible explanation for it at the present moment. Thus, we do not include benzene in the following discussion. In Table 1, we also list the Gibbs free energy change ( $\Delta G$ ) obtained from the equation  $\Delta G = -RT \ln K_f$  at 293 K. A good correlation between  $\Delta G$  and  $\epsilon_r$  is clear, which suggests that the solvation affects  $\Delta G$  in the BPK/amine complex formation. In the next section, we consider solvation energy, which depends on  $\epsilon_r$ .

**3.4. Thermodynamic Analysis of Complex Formation Reaction.** **3.4.a. Solvation Energy.** An Onsager's reaction field model<sup>32–34</sup> is introduced to estimate solvation energy. This model describes solute/solvent interaction as a function of  $\epsilon_r$  and  $n$  (refractive index) of solvent. The reaction field model expresses solvation energy by

$$\Delta E_{\text{sol}} = \frac{2\mu^2}{r^3} \left( \frac{\epsilon_r - 1}{\epsilon_r + 2} - \frac{n^2 - 1}{n^2 + 2} \right) \quad (2)$$

where  $\mu$  and  $r$  represent the dipole moment and the diameter of solute, respectively. Since the refractive indexes are essentially the same ( $n = 1.4$ ) for all the solvents, the second term of eq 2 becomes constant. Thus, solvation energy is assumed to depend only on the electrostatic term and can be expressed as a linear function of  $(\epsilon_r - 1)/(\epsilon_r + 2)$  ( $=f(\epsilon_r)$ ).

We introduce the equation  $\Delta G = \Delta G^0 - \Delta G^s$ , where  $\Delta G^0$  is Gibbs free energy change of the complex formation reaction without solvation and  $\Delta G^s$  is the additional term due to the effect of solvation. Since  $\Delta G^0$  is constant for all the solvents, we performed a trial plot of  $\Delta G$  against  $f(\epsilon_r)$  according to eq 2 for seven different solvents as shown in Figure 3 to determine if there exists any correlation between  $\Delta G$  (or  $\Delta G^s$ ) and  $\epsilon_r$ . The

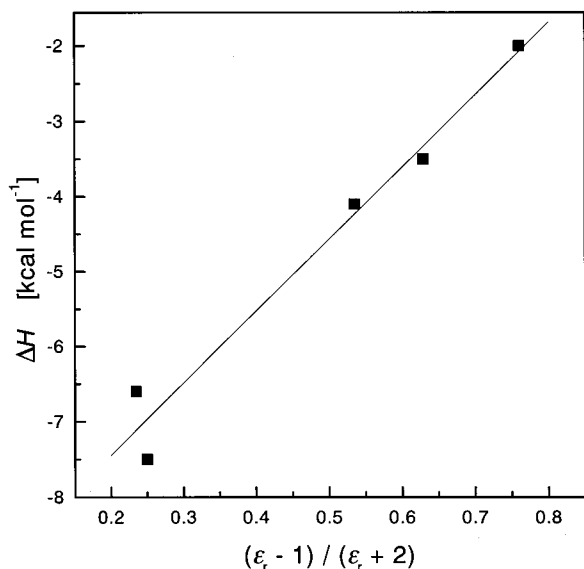


**Figure 5.** Correlation between  $\Delta H$  and  $(\epsilon_r - 1)/(\epsilon_r + 2)$ . Data are listed in Table 2 and fitted to a linear relation.

**TABLE 2: Enthalpy and Entropy Changes in BPK/TEA Complex Formation Reaction**

solvent	$f(\epsilon_r)$	$\Delta H$ [kcal mol <sup>-1</sup> ]	$\Delta S$ [cal K mol <sup>-1</sup> ]	$T\Delta S^a$ [kcal mol <sup>-1</sup> ]
cyclohexane	0.254	-7.5	-16.5	-4.83
<i>n</i> -hexane	0.229	-6.6	-13.2	-3.87
<i>o</i> -chlorotoluene	0.535	-4.1	-5.2	-1.52
<i>p</i> -chlorotoluene	0.629	-3.5	-3.4	-1.00
1,2-dichloroethane	0.764	-2.0	+1.3 <sup>b</sup>	+0.38 <sup>b</sup>

<sup>a</sup>  $T = 293$  K. <sup>b</sup> The  $\Delta S$  values were estimated from the equation  $\Delta S = (\Delta H - \Delta G)/T$  with experimental values of  $\Delta G$  at room temperature and  $\Delta H$  measured by the van't Hoff plot.

plot shows a good linear relationship. Therefore, it is concluded that  $\Delta G$  and hence  $\Delta G^s$  are controlled by  $\epsilon_r$  of the solvent after the reaction field model.

**3.4.b. Enthalpy and Entropy Changes upon Solvation.** The stabilization model by solvation seems to explain the  $\epsilon_r$  dependence of  $\Delta G$  in the BPK/TEA complex formation. Since the Gibbs free energy consists of enthalpy and entropy terms ( $\Delta G = \Delta H - T\Delta S$ ), we discuss the solvation effect by considering two terms separately and try to understand how these thermodynamic terms ( $\Delta H$  and  $\Delta S$ ) of the reaction depend on the dielectric constant of solvent.

Figure 4 shows the van't Hoff plot of  $R \ln K_f$  against  $1/T$  measured in *n*-hexane. A least-squares method was applied to fit the equation  $R \ln K_f = \Delta S - \Delta H/T$  to the data, and the  $\Delta H$  and  $\Delta S$  values were determined from the slope and the intercept, respectively. The same procedure was employed to determine  $\Delta H$  and  $\Delta S$  values in other solvents, and the resultant values are listed in Table 2.

We introduce following thermodynamic equations:

$$G_{\text{re}} = G_{\text{re}}^0 + \Delta G_{\text{re}}^s$$

$$G_{\text{com}} = G_{\text{com}}^0 + \Delta G_{\text{com}}^s$$

where  $G_{\text{re}}$  and  $G_{\text{com}}$  represent Gibbs free energies of the reactants and complex, respectively.  $G_{\text{re}}^0$  and  $G_{\text{com}}^0$  mean Gibbs free energies of the nonsolvated reactants and complex, respectively.  $\Delta G_{\text{re}}^s$  and  $\Delta G_{\text{com}}^s$  represent Gibbs free energy changes for the solvation of the reactants and complex, respectively. Thus, the

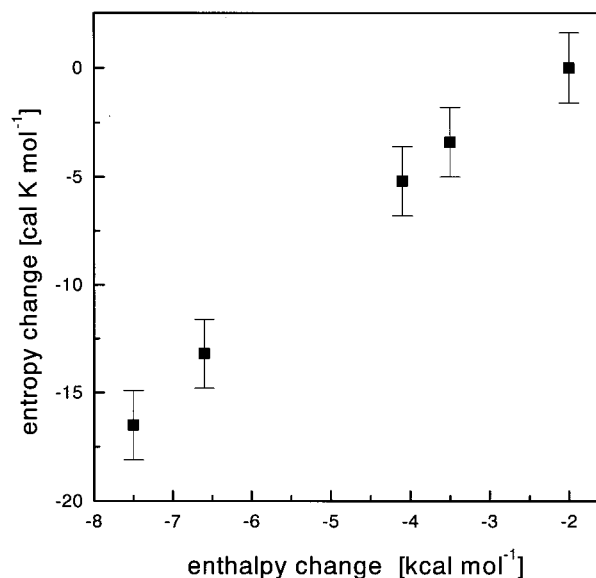
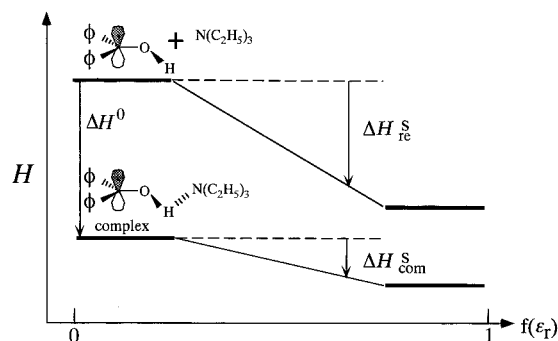


**Figure 6.** Correlation between  $\Delta H$  and  $\Delta S$ . The data are listed in Table 2.

a) enthalpy changes upon complex formation



b) entropy changes upon complex formation

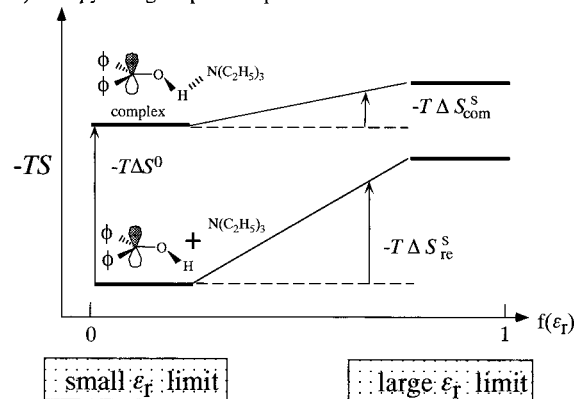


**Figure 7.** Energy diagrams of the reactants and the complex. Both  $\Delta H$  and  $T\Delta S$  are small in the solvent with relatively large  $\epsilon_r$ .

Gibbs free energy change of the complex formation reaction,  $\Delta G$ , is given by

$$\begin{aligned} \Delta G &= G_{\text{com}} - G_{\text{re}} \\ &= (G_{\text{com}}^0 - G_{\text{re}}^0) + (\Delta G_{\text{com}}^s - \Delta G_{\text{re}}^s) \\ &= \{\Delta H^0 + (\Delta H_{\text{com}}^s - \Delta H_{\text{re}}^s)\} - T\{\Delta S^0 + \\ &\quad (\Delta S_{\text{com}}^s - \Delta S_{\text{re}}^s)\} \end{aligned}$$

In the enthalpy term, the second term is for the solvation energy

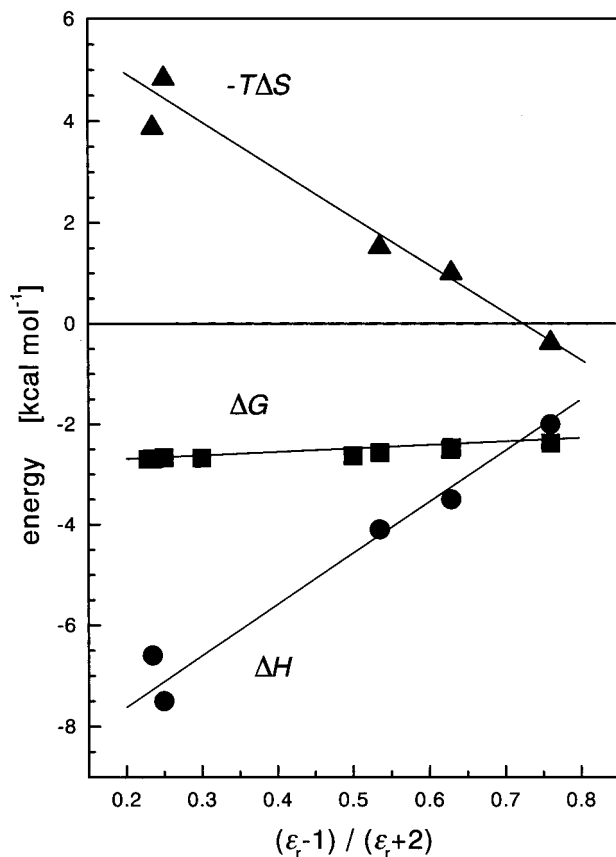


Figure 8. Correlation of  $\Delta H$ ,  $\Delta G$ , and  $-T\Delta S$  to  $(\epsilon_r - 1)/(\epsilon_r + 2)$ .

and possibly in proportion to  $f(\epsilon_r)$ . Since the first term is constant for all solvents, we plot the  $\Delta H$  values against  $f(\epsilon_r)$  in Figure 5 to find some correlation between  $\Delta H$  and  $\epsilon_r$ . Figure 5 shows a good linear dependence of  $\Delta H$  upon  $f(\epsilon_r)$ . Therefore, it is concluded that  $\Delta H$  is controlled by  $\epsilon_r$  of the solvent, and the reaction field model seems valid in the complex formation  $\text{BPK} + \text{TEA} \rightarrow \text{complex}$ . Since the slope in the plot of  $\Delta H$  vs  $f(\epsilon_r)$  is positive as seen in Figure 5, the solvation energy of the reactants is larger than that of the complex. We roughly discuss this result according to eq 2. Since the refractive index  $n$  and the dielectric constant  $\epsilon_r$  of each solvent are constant, we consider only part of  $\mu^2/r^3$ . This formula means that the solvation energy depends on the dipole moment and the volume. We discuss these factors separately. The volumes of BPK and TEA are smaller than the complex. Thus, the solvation energy for the reactant is larger than that of the complex. It is rather complicated to explain the result by considering the dipole moment effect because the dipole moment of the complex can be larger or smaller depending on the structure of the complex. If the dipole moment plays an important role in the solvation, the complex should have smaller dipole moment. Thus, the dipoles of BPK and TEA may be antiparallel to cancel each other in the complex. We have no information about the dipole moment of the complex, and it is difficult to conclude which factor is important.

The  $\Delta S$  values, which are negative in the association reaction of the present interest, apparently depend on  $\epsilon_r$  and change from  $-16.5$  to nearly zero [ $\text{cal K mol}^{-1}$ ] as  $\epsilon_r$  increases from 1.9 to 10.7. We qualitatively discuss the relation between enthalpy change ( $\Delta H^\circ$ ) and entropy change ( $\Delta S^\circ$ ) by solvation, since there is no theory to analyze the dependence of  $\Delta S$  on  $\epsilon_r$  quantitatively.

$\Delta H$  values are plotted against  $\Delta S$  in Figure 6. The absolute value of  $\Delta H$  (or exothermicity of the reaction) increases as the entropy change decreases, which indicates that solvation controls not only  $\Delta H$  but also  $\Delta S$ . When the solvent has negligibly small  $\epsilon_r$ , the enthalpy changes of solvation  $\Delta H^\circ$  for the reactants and the complex are negligible and the solvent molecules are loosely bounded to the reactants and the complex. Thus, the solvent molecules are not well aligned with the reactants and also with the complex (negligible  $\Delta S^\circ$ ). This is the case of the "small  $\epsilon_r$  limit" illustrated in Figure 7, and the free energy change is expressed by  $\Delta G^0 = \Delta H^0 - T\Delta S^0$ . On the other hand, in the polar solvent having large  $\epsilon_r$ , the solvation energy becomes much larger according to Onsager's reaction field model (negative and larger  $\Delta H^\circ$ ) and the solvent molecules are tightly trapped by the reactants and the complex. Thus, the solvent molecules are well aligned with the reactants and with the complex (negative and large  $\Delta S^\circ$ ). This is the case of the "large  $\epsilon_r$  limit" in Figure 7. As a result, absolute magnitudes of  $\Delta H$  and  $\Delta S$  values decrease when  $\epsilon_r$  changes from the small  $\epsilon_r$  limit to large  $\epsilon_r$  limit. It might be worthy of note that (1) both  $\Delta H$  and  $T\Delta S$  contribute comparably to  $\Delta G$  (see Table 2) and that (2) these contributions cancel out each other, resulting in a rather constant  $\Delta G$  value against  $\epsilon_r$  (see Table 1). This feature is visualized in Figure 8 where  $\Delta G$ ,  $\Delta H$ , and  $-T\Delta S$  were plotted against  $f(\epsilon_r)$  values; the  $\Delta H$  and  $T\Delta S$  contributions greatly vary, but the apparent formation constant (or  $\Delta G$ ) does not vary greatly for various solvents with different  $\epsilon_r$ . All these phenomena can be reasonably explained in the thermodynamical terms described above.

**Acknowledgment.** The present work is partly defrayed by a Grant-in-Aid for Scientific Research (No. 06453018) and Priority-Area-Research on "Photoreaction Dynamics" (No. 06239103) from the Ministry of Education, Science, Sports and Culture of Japan.

## References and Notes

- (1) Cohen, S. G.; Chao, H. M. *J. Am. Chem. Soc.* **1968**, *90*, 165.
- (2) Guttenplan, J. B.; Cohen, S. G. *J. Am. Chem. Soc.* **1972**, *94*, 4040.
- (3) Arimitsu, S.; Masuhara, H. *Chem. Phys. Lett.* **1973**, *22*, 543.
- (4) Miyasaka, H.; Mataga, N. *Bull. Chem. Soc. Jpn.* **1990**, *63*, 131.
- (5) Miyasaka, H.; Morita, K.; Kamada, K.; Mataga, N. *Bull. Chem. Soc. Jpn.* **1990**, *63*, 3385.
- (6) Miyasaka, H.; Morita, K.; Kamada, K.; Mataga, N. *Chem. Phys. Lett.* **1991**, *178*, 504.
- (7) Miyasaka, H.; Kiri, M.; Morita, K.; Mataga, N.; Tanimoto, N. *Chem. Phys. Lett.* **1992**, *199*, 21.
- (8) Devadoss, C.; Fessenden, R. W. *J. Phys. Chem.* **1990**, *94*, 4540.
- (9) Arimitsu, S.; Masuhara, H.; Mataga, N.; Tsubomura, H. *J. Phys. Chem.* **1975**, *79*, 1255.
- (10) Inbar, S.; Linschitz, H.; Cohen, S. G. *J. Am. Chem. Soc.* **1980**, *102*, 1419.
- (11) Bhattacharya, K.; Das, P. K. *J. Phys. Chem.* **1986**, *90*, 3987.
- (12) Hoshino, M.; Shizuka, H. *J. Phys. Chem.* **1987**, *91*, 714.
- (13) Kajii, Y.; Fujita, M.; Hiratuska, H.; Obi, K.; Mori, Y.; Tanaka, I. *J. Phys. Chem.* **1987**, *91*, 2791.
- (14) Beckett, A.; Porter, G. *Trans. Faraday Soc.* **1963**, *59*, 2038.
- (15) Broberg, A.; Meisel, D. *J. Phys. Chem.* **1985**, *89*, 2507.
- (16) Bartholomew, R. F.; Davidson, R. S.; Lambeth, P. F.; McKellar, J. F.; Turner, P. H. *J. Chem. Soc., Perkin. Trans. 2* **1972**, 577.
- (17) Land, E. J. *Proc. R. Soc. A* **1968**, *305*, 457.
- (18) Ichikawa, T.; Ishikawa, Y.; Yoshida, H. *J. Phys. Chem.* **1988**, *92*, 508.
- (19) Griller, D.; Howard, J. A.; Marriott, P. R.; Scaiano, J. C. *J. Am. Chem. Soc.* **1981**, *103*, 619.
- (20) Matsushita, Y.; Kajii, Y.; Obi, K. *J. Phys. Chem.* **1992**, *96*, 4455.
- (21) Matsushita, Y.; Kajii, Y.; Obi, K. *J. Phys. Chem.* **1992**, *96*, 6566.
- (22) Davidson, R. S.; Wilson, R. *J. Chem. Soc. B* **1970**, 71.
- (23) Obi, K.; Yamaguchi, H. *Chem. Phys. Lett.* **1978**, *54*, 448.

- (24) Hiratsuka, H.; Yamazaki, Y.; Maekawa, Y.; Hikida, T.; Mori, Y. *J. Phys. Chem.* **1986**, *90*, 774.
- (25) Nagarajan, V.; Fessenden, R. W. *Chem. Phys. Lett.* **1984**, *112*, 207.
- (26) Kajii, Y.; Itabashi, H.; Shibuya, K.; Obi, K. *J. Phys. Chem.* **1992**, *96*, 7244.
- (27) (a) Kawai, A.; Kobori, Y.; Obi, K. *Chem. Phys. Lett.* **1993**, *215*, 203. (b) Kawai, A.; Aoki, A.; Kobori, Y.; Obi, K. *J. Phys. Chem.* **1996**, *100*, 10021.
- (28) Terazima, M.; Okamoto, K.; Hirota, N. *J. Phys. Chem.* **1993**, *97*, 13387.
- (29) Takeda, K.; Kajii, Y.; Shibuya, K.; Obi, K. *J. Photochem. Photobiol. A* **1998**, *115*, 109.
- (30) Tramer, A.; Zaborowska, M. *Acta Phys. Pol.* **1968**, *34*, 821.
- (31) Mataga, N.; Kubota, T. *Molecular Interactions and Electronic Spectra*; Marcel Dekker: New York, 1970.
- (32) Onsager, L. *J. Am. Chem. Soc.* **1936**, *58*, 1486.
- (33) Wilson, J. N. *Chem. Rev.* **1939**, *25*, 377.
- (34) McRae, E. G. *J. Phys. Chem.* **1957**, *61*, 562.
- (35) For examples, see the following. (a) Nagakura, S. *J. Am. Chem. Soc.* **1958**, *80*, 520. (b) Bhowmik, B. B.; Chattopadhyay, S. *Spectrochim. Acta* **1981**, *37A*, 445.
- (36) Levin, R. D.; Lias, S. G. Ionization Potential and Appearance Potential Measurements, 1971–1981. *Natl. Stand. Ref. Data Ser. (U.S., Natl. Bur. Stand.)* **1982**, *71*.